2024 IEEE International Conference on Robotics and Automation (ICRA 2024)
May 13-17, 2024. Yokohama, Japan

Crosstalk-Free Impedance-Separating Array Measurement for Iontronic Tactile Sensors*

Funing Hou, Gang Li, Chenxing Mu, Mengqi Shi, Jixiao Liu, *Member IEEE*, Shijie Guo, *Member IEEE*

***Abstract*— Iontronic tactile sensors are promising to measure spatial-temporal contact information with high performance. However, no suitable measuring method has been presented, due to issues with crosstalk and non-negligible equivalent resistance. Hence, this study presents an impedance-separating method, which does not require complex analog components. A general Quadri-Terminal Impedance Network (QTIN) model is introduced to reduce crosstalk, which has specific compatibility with the impedance-separating method. The precise ranges are measured, showing non-rectangle shapes suitable for the response of iontronic tactile sensors. A simple denoising method is provided to reduce initial array noise obviously. This work could benefit various scenarios, such as human-robot interaction and physiological information monitoring.**

I. Introduction

Tactile sensors are essential for robots to understand and interact with the physical world. As large-area flexible sensitive arrays, tactile sensors can acquire spatial-temporal contact information. They have enabled various robotic applications including collision detection[1], material recognition [2], and human-robot interaction [3]. The characteristics of a tactile sensor have two key factors: the wiring manner and the electrical principle.

Regarding the first factor (wiring manner), the individual unit approach is an intuitive design and ideal for signal quality [4]. In this approach, each sensing unit independently connects with the readout circuit, theoretically eliminating crosstalk among adjacent units. However, the sensing area and the spatial resolution are limited due to the large number of ports and the occupied area for wires. Another promising method is electrical impedance tomography (EIT), which distributes electrodes around the tactile sensor's edge. With a few electrodes, EIT can obtain global tactile information without any wire in the sensing area. However, EIT had severe intrinsic interference, making it difficult to quantitatively correlate the output response with applied pressure [5].

Currently, the crossing-electrode form is the most popular scheme due to its simple structure, cost-efficient fabrication, and programmable sensing geometry [6], [7]. However, crosstalk is a major issue of this scheme since adjacent units share row and column electrodes. When acquiring information arrays, this interference is often overlooked, hinting that simply dividing the middle layer into individual units is insufficient for noise cancellation [8]. The zero potential method (ZPM) has proven effective in reducing crosstalk and is now widely used for measuring piezoresistive tactile sensors. However, the working principle of ZPM is based on theoretical calculations without physical interpretation [9]. This lack of guidance limits applying ZPM to other electrical principles like capacitive and iontronic. This study shows the limitations of concurrent measuring methods with ZPM.

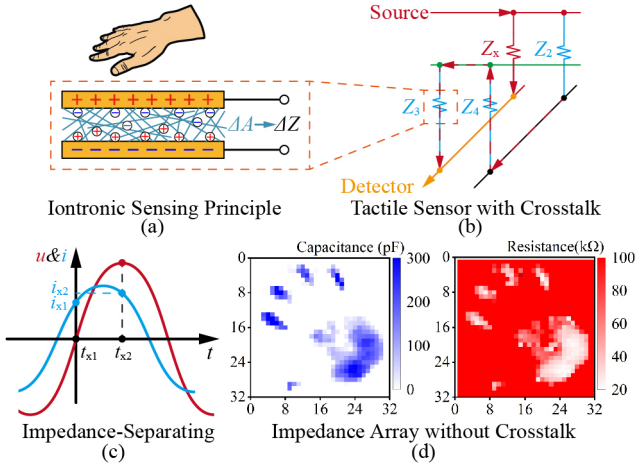

Fig. 1. Crosstalk-free iontronic tactile sensing. (a)-(b) Iontronic sensing array with crosstalk. (c)-(d) Impedance separation without crosstalk.

Regarding the second factor (electrical principle), the piezoresistive principle is the most common solution, due to the real-time direct current (DC) measurement and convenient resistance transduction [10]. However, piezoresistive output couples pressure and temperature effects [11]. In contrast, the temperature-insensitive capacitive principle is more stable in measuring pressure [12]. However, the capacitance response of conventional capacitive sensors is too weak for precise measurement. Then, iontronic supercapacitive tactile sensors have been developed with hundreds of times greater sensitivity than conventional capacitive sensors [13].

However, an essential feature of iontronic supercapacitors is equivalent serial resistance [14], although the capacitance is preferred for the linear response to pressure [6]. Hence, a necessary process is to measure capacitance and resistance separately. When measuring an iontronic unit, using LCR meters is a typical impedance-separating manner. Additionally, combined with analog computational components and low pass filters (LPFs), various impedance-separating circuits were designed for lossy capacitors) [15]-[17]. However, those methods cannot directly measure sensitive arrays, so they require an additional switcher (multiplexer) for multichannel capability [18]. The spliced system has a substantial size, a low scanning frequency, and limited crosstalk handling. These constraints restrict applications of iontronic tactile sensors.

*Corresponding authors: Shijie Guo; Jixiao Liu.
Funing Hou and Shijie Guo are with the Academy for Engineering and Technology, Fudan University, Shanghai, 200433, China (email: fnhou22@m.fudan.edu.cn, guoshijie@fudan.edu.cn).
Jixiao Liu, Gang Li, Chenxing Mu, and Mengqi Shi are with the School of Mechanical Engineering, Hebei University of Technology, Tianjin 300401, China (email: liujixiao@hebut.edu.cn, 202131404017@stu.hebut.edu.cn, 202221202103@stu.hebut.edu.cn, mengqishi_hebut@163.com).

As alternative methods, condensance (capacitive reactance) voltage dividing [19] and charge-discharge [20] are the currently embedded methods to measure the capacitance array of iontronic tactile sensors. In these methods, resistance was ignored during measuring, based on the assumption that the resistance decreases sharply with increasing applied pressure. However, by measuring the phases of alternative current (AC) impedance, this study finds that the resistance cannot be ignored and shows the inadequacy of using these methods to measure iontronic tactile sensors.

To address the challenges of measuring crosstalk-free impedance-separated arrays for crossing-electrode iontronic tactile sensors, this study presents a novel approach as shown in Fig. 1. The key contributions are:

- Demonstrating the non-negligible influence of resistance when measuring iontronic tactile sensors. Then, an impedance-separating method is proposed, using samples at two specific moments, without complex analog calculating components.
- Introducing a general Quadri-Terminal Impedance Network (QTIN) model to interpret ZPM, which reveals the specific compatibility between this impedance-separating principle and ZPM.
- Presenting a simple impedance array denoising method for measuring iontronic tactile sensors, which could obviously remove the initial noise.

Compared with concurrent measuring methods for iontronic tactile sensors [18]-[20], this work realizes crosstalk-free impedance separation, which improves the precision and the reliability of using iontronic tactile sensors for various scenarios such as human-robot interaction and physiological information monitoring.

II. Iontronic Feature

A. Iontronic Equivalent Model

As shown in Fig. 2(a), the structure of an iontronic sensitive unit is sandwiched with two electrodes and an ionic film, which can form a pair of electrical double-layer capacitors (EDLCs). The applied pressure p causes an increase in internal area A, which changes the impedance Z_x. As shown in Fig. 2(b), Z_x can be serially equivalent to a capacitance C_x and a resistance R_x. The detailed fabrication and the fundamental sensing principle were in our previous work [6].

B. Response with Pressure and Frequency

As shown in Fig. 2(c), the width of each electrode was set to 5 mm. The ionic film was composed of polyvinylidene fluoride, trifluoromethyl sulfonyl imide, and dimethylacetamide in a mass ratio of 13: 4: 68. Response tests were performed using a material test system (MTS, ZQ-990B) and an LCR meter (IM3536). The measuring sinusoid voltage amplitude of the LCR meter was set to 1.74V, which matched the amplitude of the homemade signal generator in Fig. 3(a).

As plotted in Fig. 2(d)-(e), both the capacitance C_{LCR} and the resistance R_{LCR} decreased with increasing measuring frequency f_{LCR}. However, increasing applied pressure p caused C_{LCR} to increase while R_{LCR} to decrease. While measuring iontronic tactile sensors, researchers tend to ignore the resistive response due to the sharp decrease in resistance with increasing pressure. Hence, an intuitive assumption was that the precise capacitive value could be obtained using pure-capacitor measuring methods (such as charge-discharge), regardless of the resistance.

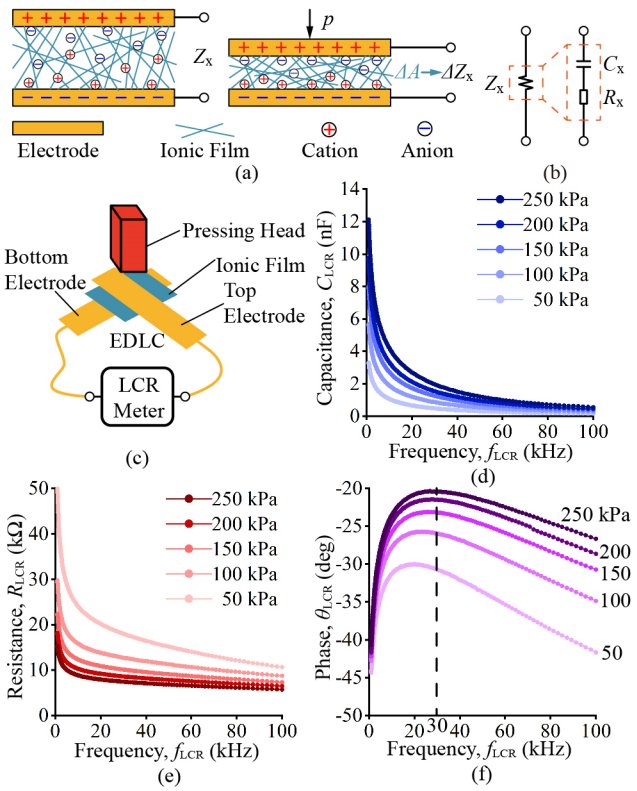

Fig. 2. Iontronic response with applied pressure and measuring frequency. (a) The sensitive unit impedance Z_x changes with the internal contacting area A, due to the pressure p. (b) Equivalent model of a sensitive unit. (c) Experimental setup. (d)-(f) Response of capacitance, resistance, and phase.

However, as shown in Fig. 2(f), within the entire measuring range of the pressure (50 to 250 kPa) and the frequency (1 to 100 kHz), the phase θ_{LCR} remained above -45°, which indicates the resistance is consistently greater than the condensance, that is the influence of resistance to measuring current is more than capacitance. Hence, the resistance cannot be ignored when measuring iontronic tactile sensors.

Additionally, Fig. 2(f) shows that at f_{LCR} = 30 kHz, θ_{LCR} were relatively stable over varying measuring frequencies (insensitive to frequency disturbance). Therefore, this study chose 30 kHz as the measuring frequency.

III. Impedance Separation

Due to the non-negligible resistance, we require an impedance-separating method to measure iontronic tactile sensors precisely. Rather than relying on complex analog calculating components or analyzing the entire signal, this study presents a simple measuring principle, which is feasible for performance-limited chips, low-power-consuming devices, or cost-efficient applications.

A. Measuring Principle

As shown in Fig. 3(b), u_0 is a sinusoid source (with a period T_s and an amplitude u_{0m}) applied to Z_x, and i_x is the current of Z_x. Then, the currents at two moments ($t_{x1} = 0$ and t_{x2}

= $T_s/4$) are detected, denoted as i_{x1} and i_{x2}, which allow to calculate C_x and R_x as follows:

The i_x can be expressed as

$$i_x = u_0 / Z_x = u_0 / (R_x - jX_x) \quad (1)$$

where X_x is the condensance of C_x.

According to (1), the phase θ_x and the current amplitude i_{xm} can be obtained as

$$\tan\theta_x = -X_x / R_x ; i_{xm} = u_{0m} / \sqrt{R_x^2 + X_x^2} \quad (2)$$

The two sampled currents were

$$i_{x1} = i_{xm} \sin(0-\theta); i_{x2} = i_{xm} \sin(\pi/2-\theta) \quad (3)$$

According to (3), θ_x and i_{xm} can also be expressed as

$$\tan\theta = -i_{x1} / i_{x2}; i_{xm} = -i_{x1} / \sin\theta \quad (4)$$

Then, R_x and C_x can be obtained as

$$\begin{cases} R_x = \dfrac{u_{0m}}{i_{xm}}\sqrt{\dfrac{1}{1+\tan^2\theta}} = \dfrac{u_{0m}|i_{x2}|}{i_{x1}^2 + i_{x2}^2} \\ C_x = \dfrac{1}{2\pi f_s X_x} = \dfrac{1}{2\pi f_s R_x \tan\theta} = \dfrac{i_{x1}^2 + i_{x2}^2}{2\pi f u_{0m}|i_{x1}|} \end{cases} \quad (5)$$

B. Hardware Realization

The specific requirement of the proposed method is the precise temporal alignment between the sampled i_x and u_0. However, commercial signal generators find it difficult to track u_0 along with time. Hence, as shown in Fig. 3(a), this study designed a sinusoidal signal generator (SSG) for converting the DC square signal u_p to the AC sinusoidal signal u_0. In SSG, C_b of 2.2 nF was served to block the DC component of u_p. Then, two LPFs filtered u_p to generate u_0 (the detailed filtering principle was presented in our previous work [19]). The component parameters of LPFs require manual tuning for precise output.

As shown in Fig. 3(c), u_p was generated by a microcontroller (MCU; STM32H7VI here) timer comparator output. Then, this study uses the standard deviation σ to quantitatively evaluate the generated sinusoidal signals. The σ of our previous work is 0.46 V[19], and the σ of a commercial signal generator (AFG1062) is 0.02 V. Although higher than the commercial signal generator, the σ of this study was confined to 0.04 V. Additionally, the generated u_0 is temporally aligned with u_p, enabling the timer to provide a time standard to track u_0.

Then, as shown in Fig. 3(a), i_x was converted to voltage u_x by a trans-impedance amplifier (TIA) with a sampling resistance R_0. R_0 was the minimum Z_x that the circuit could measure, because a less Z_x would cause u_x to exceed the MCU analog-to-digital converter (ADC) range. The u_x sampling moments could be conveniently fixed by setting the timer.

IV. Crosstalk-Free Measurement

Crosstalk is a common issue for crossing-electrode tactile sensors. However, currently, there is no suitable solution for iontronic tactile sensors, because the crosstalk requires to be reduced while separately measuring impedance.

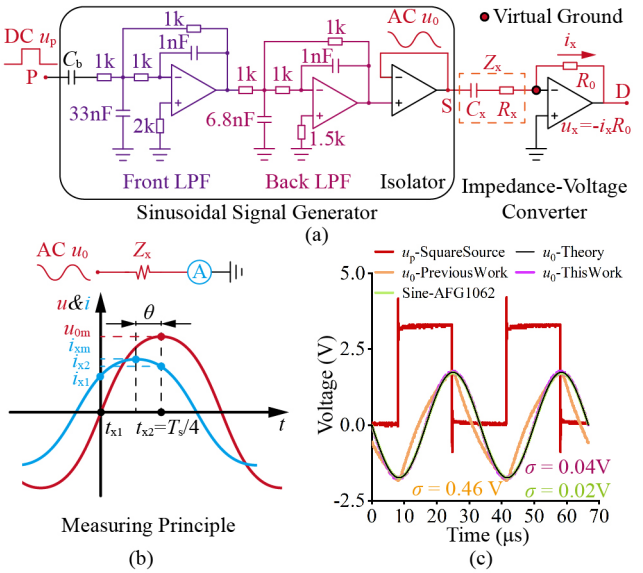

Fig. 3. Impedance-separating method. (a) Signal converting principle. (b) Fundamental measuring principle. (c) Signal output and evaluation.

A. Visualizing Crosstalk

Fig. 4(a)-(b) shows a 2 × 2 instance, where Z_x is the target measuring unit, but the measuring current can bypass Z_x along the shunting branch. This crosstalk mechanism is well-known for piezoresistive tactile sensors. However, there has not been an intuitive phenomenon to verify this mechanism or assess crosstalk-reducing methods. Hence, this study visualized crosstalk using a 5 × 5 array with halogen bulbs (Philips, 12 V) shown in Fig. 4(d). A black heat-shrink tube was wrapped around each bulb to isolate light among individual bulbs.

Fig. 4(e) is the general current branch topology when measuring $Z_{i,j}$. The labels (Z_x, Z_2, Z_3, and Z_4) were equivalent to the primary circuit in Fig. 4(b). The units with the same row ($Z_{i,:}$) or column ($Z_{:,j}$) were on higher-current main circuits, while other units were on the lower-current branch circuits. This causes the cross pattern in Fig. 4(d).

To reduce crosstalk, as shown in Fig. 4(f)-(g), this study presented QTIN to interpret ZPM. The core thought of ZPM is to connect unworking electrodes to the same potential ($r_:$ to r_p and $c_:$ to c_p), which typically is the ground. Hence, QTIN had four terminals (r_x, c_x, r_p, and c_p) to connect the readout circuit.

B. Limitations of Concurrent Methods

1) Voltage Dividing Method

Utilizing a sampling impedance Z_0 is a simple measuring principle to measure the divided voltage [19]. Theoretically, the impedance separation could be completed by detecting the entire output signal [21] (but these works did not realize this function, which just measured capacitance by ignoring resistance for fast measuring), and various pressure representations could be obtained using this method [7], [22], [23]. However, as shown in Fig. 5(a)-(b), Z_3 would bypass Z_0 and affect the sampling signal u_x. Additionally, as a combination of sensing units, Z_3 was unstable while the tactile sensor was working, resulting in an unpredictable u_x error.

2) Charge-Discharge Method

As shown in Fig. 5(c), the crosstalk-free charge-discharge method for tactile sensors [20] could also be analyzed using the QTIN, which could obtain Z_x by thrice measurements,

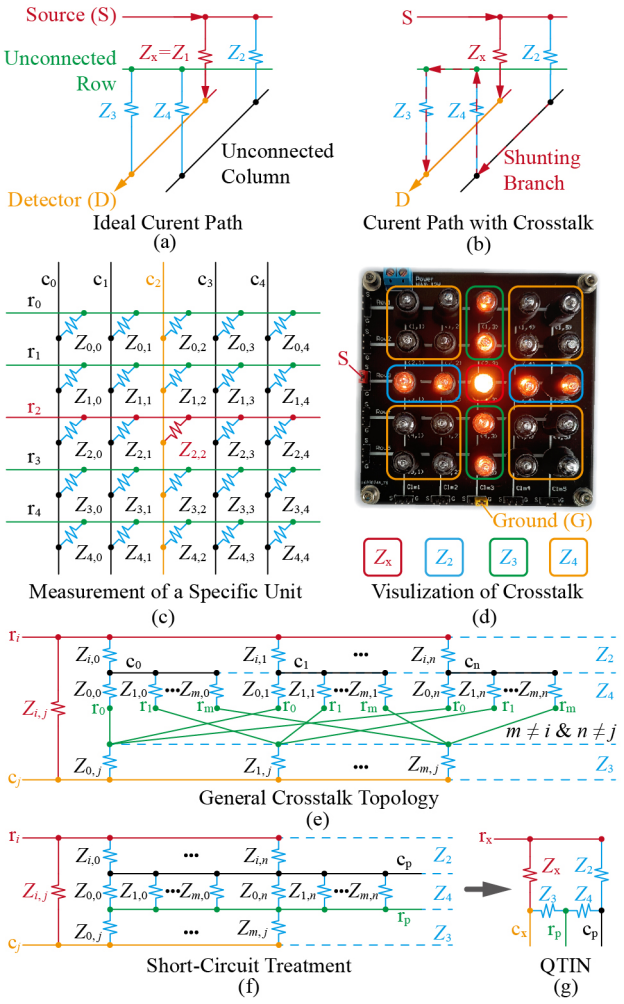

Fig. 4. Crosstalk mechanism. (a)-(b) The measuring current can bypass the target unit Z_x along the shunting branch. (c)-(e) Crosstalk of a 5 × 5 array. (f)-(g) Quadri-Terminal Impedance Network (QTIN) to address crosstalk.

denoted as Z_i, Z_{ii}, Z_{iii}:

$$Z_i = Z_x // Z_2;\ Z_{ii} = Z_2 // Z_3;\ Z_{iii} = Z_x // Z_3 \tag{6}$$

However, as shown in Fig. 5(d), this study used the PCap01 chip (from the same series as [20]) to measure Z_x, where C_x was set to 100 pF. Fig. 5(e) shows that this method is only capable of measuring capacitance, and the readout C_{PCAP} would sharply decrease with increasing R_x. Additionally, while measuring several columns in parallel, this method was supposed to use the strategy in Fig. 5(f) (with two target units, Z_{x1} and Z_{x2}, as an example). Then, the relationships were

$$\begin{aligned} &Z_i = Z_{x1} // Z_{21} // Z_{x2} // Z_{22};\ Z_{ii} = Z_{21} // Z_{31} // Z_{22} // Z_{32};\\ &Z_{iii}(c_1) = Z_{x1} // Z_{31};\ Z_{iii}(c_2) = Z_{x2} // Z_{32} \end{aligned} \tag{7}$$

However, Z_{x1} and Z_{x2} could not be determined by (7), which implied that the charge-discharge method had limitations in measuring units simultaneously, resulting in a low frequency for scanning tactile sensors.

C. Scanning Parrallely Without Crosstalk

As shown in Fig. 6(a)-(b), the virtual ground of the TIA shorted Z_3 and Z_4. Hence, no current influenced the measuring i_x. That is, the impedance-separating could measure tactile sensors without crosstalk.

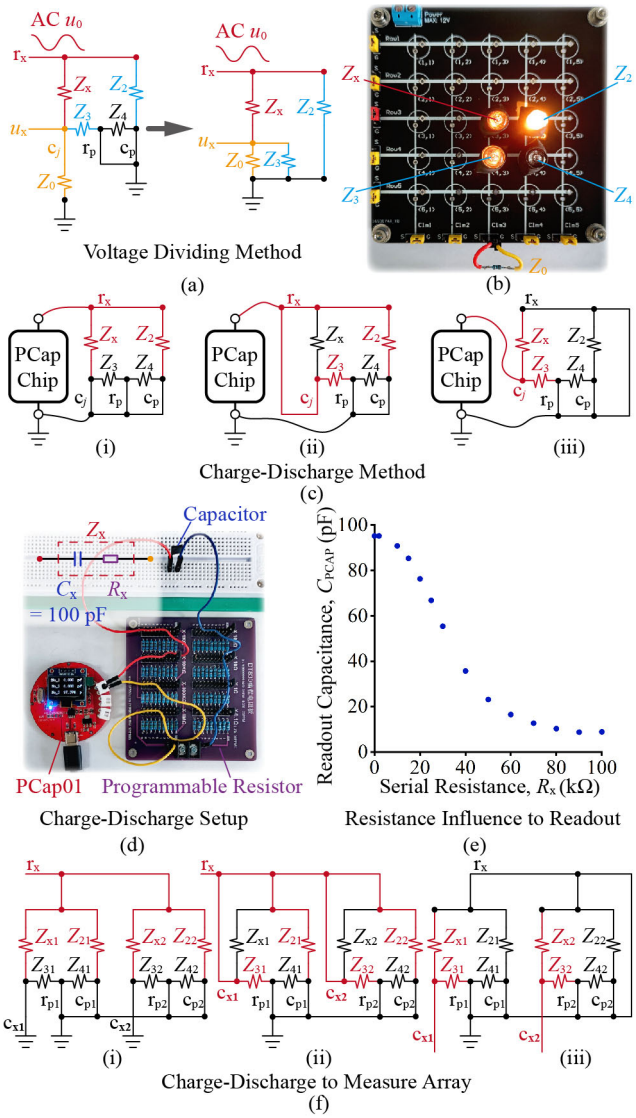

Fig. 5. Measurement of concurrent methods. (a)-(b) In voltage dividing method, Z_3 would affect sampling. (c) Thrice switches were required for the charge-discharge method. (d)-(e) R_x would affect the readout of C_x. (f) Multi-column measurement using the method in (c).

As shown in Fig. 6(c), amplifiers were used to isolate the on-resistor of the row (R_r) and the column (R_c) multiplexers (ADI, ADG706), and the output voltages u_x were detected by ADCs. Fig. 6(d) shows that the parallel multi-column measurement could be achieved due to no current interference among adjacent units (four parallel groups in the actual circuit). This specific compatibility between the impedance-separating method and ZMP endowed the tactile sensors with a high scanning frequency.

Additionally, as shown in Fig. 6(d), since there is no current in r_p, r_p did not need to be connected to the readout circuit, which could simplify the readout circuit design.

V. Measuring Experiments

A. Measurement for Standard Components

As shown in Fig. 8(d), this study utilized an iontronic tactile sensor with 32 × 32 units. Then, the minimum Z_x of the iontronic tactile sensor was limited to 2 kΩ, so the maximum current of a row for 32 columns was 27.8 mA, which was

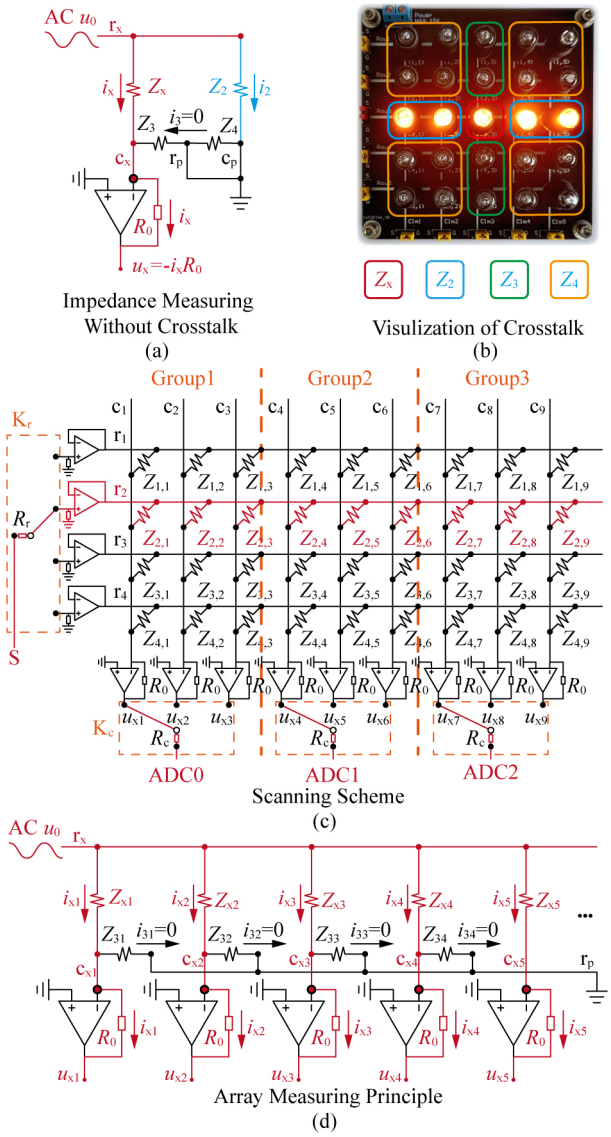

Fig. 6. Scanning principle. (a)-(b) Measuring without crosstalk. (c)-(d) Measuring parallelly.

slightly less than the maximum output current (30 mA) of an ADG706 channel. Hence, R_0 was set to 2 kΩ.

Table. I-II present the measuring errors e of C_x and R_x using standard components by

$$e = (\bar{x} - x_0) / x_0 \tag{8}$$

where $\bar{x}$ is the average of continuous 50 readouts; x_0 is the nominal value.

As shown in Fig. 7(a), different from other works testing readout circuits by directly connecting with tactile sensors (thousands of sensitive units were inconsistent and without quantitative calibration for each sensitive unit), this study designed a letter icon with standard components to test the performance of scanning impedance array. Fig. 7(b) shows the readout of our previous work [19], which could not get R_x, all the letters were coupled with each other, and the readout C_x was far less than the nominal value. Fig. 7(c) shows that, with the method in Fig. 4(c) (measuring point by point), the letters were obscured by crosstalk. Fig. 7(d) is the result using the crosstalk-free impedance-separating method, where the

TABLE I. CAPACITANCE MEASURING PRECISION

Capacitance		Standard Capacitance, C_x (nF)								
e		***0.01***	***0.1***	***0.22***	***0.47***	***0.68***	***1.0***	***2.2***	***3.3***	***4.7***
Standard Resistance, R_x (kΩ)	***2***	-0.40	0.08	0.09	0.15	0.03	0.08	0.05	-0.08	-0.05
	5	66.34	0.06	0.07	0.12	0.00	0.06	0.02	-0.12	-0.05
	10	0.82	0.03	0.04	0.09	-0.05	0.01	-0.02	-0.16	-0.11
	15	148.7	0.04	0.01	0.06	-0.06	-0.03	-0.05	-0.09	-0.12
	20	0.99	0.01	0.01	-0.01	-0.10	-0.07	-0.11	-0.25	-0.23
	25	86.47	-0.03	0.00	0.03	-0.11	-0.08	-0.16	-0.11	0.47
	30	1.37	-0.03	-0.03	-0.05	-0.19	-0.16	0.04	0.14	0.66
	40	1.25	-0.03	-0.12	-0.11	-0.26	-0.20	0.58	250.1	271.9
	50	34.15	-0.02	-0.12	-0.18	-0.23	0.16	347.0	812.7	695.6
	60	5.48	-0.08	-0.14	0.01	0.08	0.75	152.4	397.9	282.6
	70	1.68	-0.07	-0.10	0.19	0.27	417.3	660.7	342.1	454.8
	80	49.59	-0.07	-0.10	250.0	431.1	738.6	546.0	804.0	757.6
	90	646.6	-0.08	-0.06	237.9	481.0	732.1	800.1	621.0	364.8
	100	279.5	-0.04	-0.15	292.0	727.6	-0.52	142.8	36.12	41.11

Error of blue marks < ±20%

TABLE II. RESISTANCE MEASURING PRECISION

Resistance		Standard Capacitance ± 5%, C_x (nF)								
e		***0.01***	***0.1***	***0.22***	***0.47***	***0.68***	***1.0***	***2.2***	***3.3***	***4.7***
Standard Resistance ± 1%, R_x (kΩ)	***2***	62.29	-0.99	-0.64	-0.17	-0.13	-0.09	-0.04	-0.04	-0.03
	5	56.00	-1.00	-0.22	-0.08	-0.06	-0.04	-0.03	-0.03	-0.03
	10	16.63	-0.51	-0.08	-0.04	-0.04	-0.04	-0.02	-0.02	-0.02
	15	7.51	-0.08	0.00	-0.03	-0.03	-0.02	-0.02	-0.02	-0.02
	20	5.40	0.01	-0.02	-0.02	-0.03	-0.03	-0.02	-0.02	-0.02
	25	6.24	0.01	-0.03	-0.01	-0.03	0.01	-0.02	-0.01	-0.01
	30	3.45	-0.02	0.00	-0.03	0.00	-0.02	-0.02	-0.01	-0.02
	40	2.07	-0.04	-0.02	0.01	0.00	0.00	-0.01	-0.01	-0.01
	50	1.49	0.03	-0.01	-0.02	-0.01	0.00	-0.01	-0.02	-0.02
	60	3.28	0.00	0.00	0.03	0.03	0.03	0.02	0.01	0.01
	70	1005	0.03	-0.02	0.02	0.01	0.01	0.00	-0.01	-0.01
	80	2.45	0.05	0.02	0.01	0.02	0.00	-0.02	-0.03	-0.04
	90	888.4	0.06	0.01	0.03	0.02	-0.01	-0.02	-0.02	-0.04
	100	0.74	0.06	-0.09	-0.04	-0.04	-0.08	-0.05	-0.04	-0.03

Error of red marks < ±10%

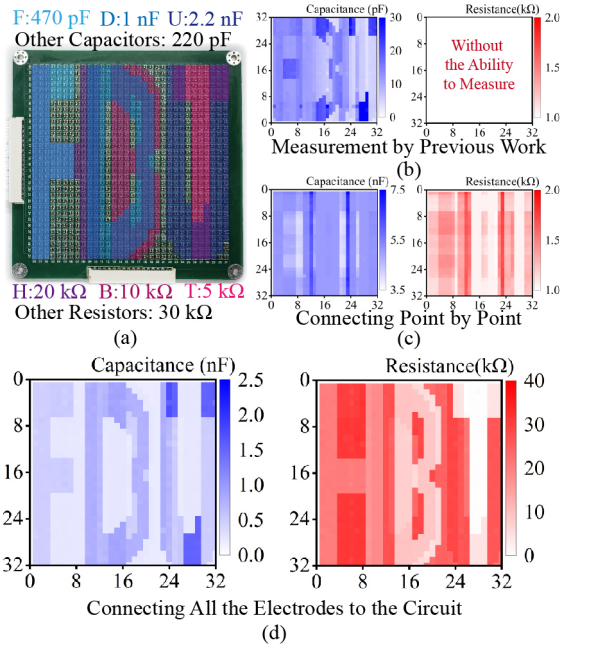

Fig. 7. Measuring impedance icon. (a) A 32 × 32 impedance array with standard components. (b)-(d) Comparing with other methods, the presented method could separately measure impedance without crosstalk.

measuring error was consistent with Table. I-II. Then, the letters were displayed clearly.

B. *Measurement for Iontronic Tactile Sensors*

As shown in Fig. 8(a), according to Table. I-II, contrasting with other impedance-separating methods [15]-[17], the precise area of either capacitance (*C* area) or resistance (*R* area) of this work was not rectangular. Additionally, the precision features of *C* and *R* areas differed, where the range of the

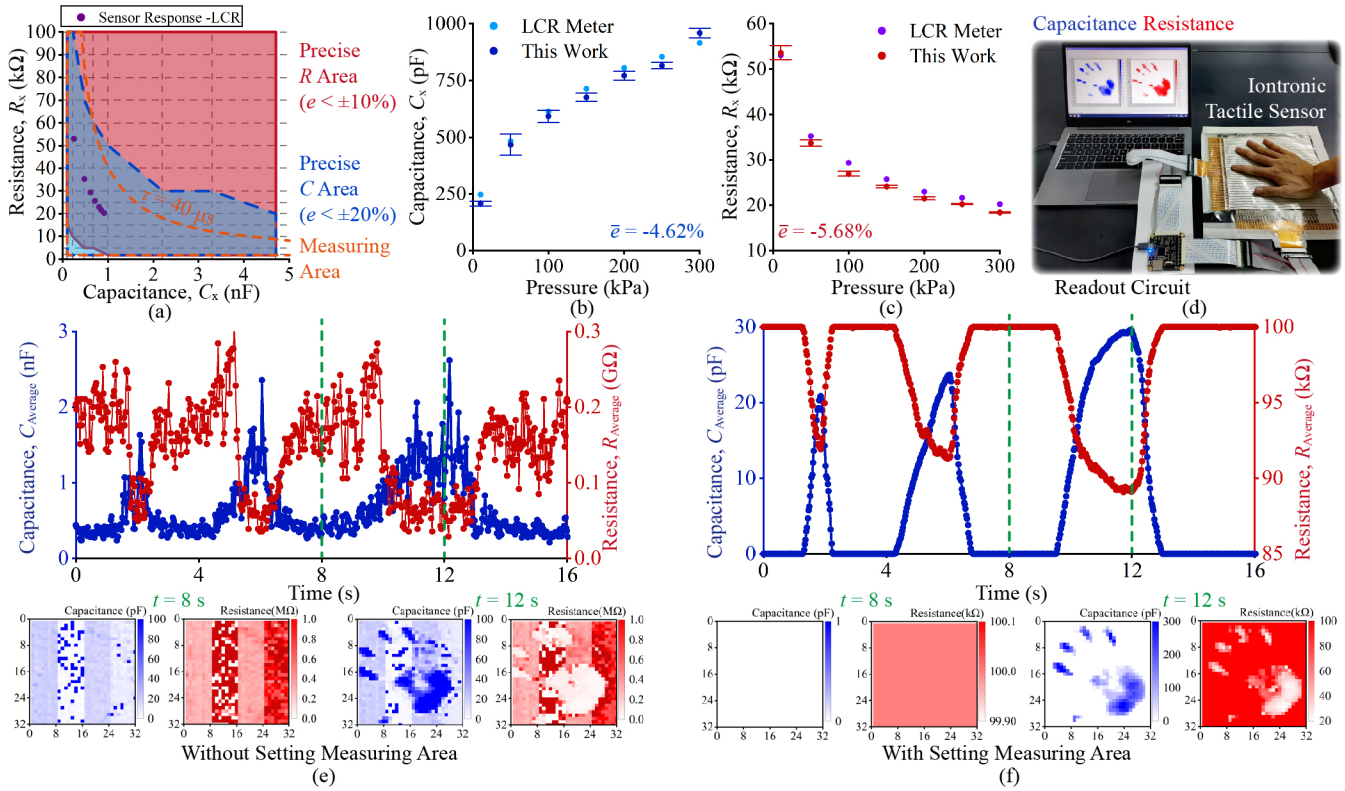

Fig. 8. Measuring iontronic tactile sensors. (a) Pressure response was in the precise area. (b)-(c) The measuring results of this work are similar to the commercial LCR meter. (d)-(e) The noise of the area without pressure was severe. (f) Denoising effect by setting measuring area.

precise *R* area was wider than the precise *C* area, but *C* was more precise than *R*, while both R_x and C_x were small. Notably, the pressure response of the iontronic tactile sensor was in both the precise areas, which shows special-shape precise areas could also be suitable for measuring tactile sensors.

As shown in Fig. 8(b)-(c), for the same test specimen with the structure in Fig. 2(c), the measured pressure response of this work was closely similar to that of the commercial LCR meter. Here, $\bar{e}$ was the average error of the seven pressures with this work, where LCR results were the ground truth.

As shown in Fig. 8(d), a subject pressed the iontronic tactile sensor thrice at varying speeds and pressures. Fig. 8(e) shows the average response of all the sensing units, where severe array noise was observed.

C. *Denoising Impedance Array*

The reason for the noise was that when no pressure was applied to a specific sensitive unit (in its initial state), its R_x was large (370 kΩ), and C_x was small (9 pF). The circuit could not measure precisely, as shown in Table I-II. Hence, as shown in Fig. 8(a), this study defined a measuring area as

$$\hat{R}_x > 100\,\text{k}\Omega;\ \hat{C}_x < 10\,\text{pF};\ \hat{\tau} = \hat{R}_x \cdot \hat{C}_x < 40\,\mu\text{s} \qquad (9)$$

Any result beyond this measuring area was considered as *Overload* (displaying R_x = *100 kΩ* and C_x = *0 pF*). As shown in Fig. 8(f), after setting the measuring area, the noise was reduced obviously.

However, as shown in Fig. 8(a), the measuring area included imprecise areas and excluded a large precise area. In the future, the measuring error principle will be investigated, and then a more reasonable denoising method will be designed with analyzing the working effect, such as minimum detectable pressure, range, and real-time performance.

Table III shows that, although the measuring frequency of this work (requiring waiting for signals to get stable) was lower than the voltage dividing method, the crosstalk-free impedance separation was achieved.

VI. Conclusions

This study presented a crosstalk-free impedance separating method for iontronic tactile sensors. Using a two-sample measuring-separating principle, we obtained precise resistance and capacitance results. The crosstalk-free performance of measuring impedance arrays was verified using an icon with standard components. Additionally, by setting a simple measuring area, the initial noise of measuring the iontronic tactile sensor was reduced obviously.

In the future, additional performances of combining the tactile sensor with the readout circuit will be tested, such as hysteresis and stability. The generalization of the readout circuit will be tested on tactile sensors with various ionic concentrations. A more suitable array denoising method will be designed to enhance comprehensive performance.

TABLE III. Comparison with Concurrent Works for Iontronic Tactile Sensors

Measuring Performance	R_x	C_x	Cross-talk-free	Parallelly Measure	Hardware Complexity	Frequency (Units per Second)
LCR Meter [18]	√	√	-	-	Commercial	0.5
Divide Voltage [19]	-	√	-	√	Simple	100 k
Charge-Discharge [20]	-	√	√	-	Complex	2 k
This Work	√	√	√	√	Simple	25 k

REFERENCES

[1] Z. Ye, G. Pang, K. Xu, et al. "Soft robot skin with conformal adaptability for on-body tactile perception of collaborative robots," IEEE Robot. Automat. Letters, vol. 7, no. 2, pp. 5127-5134, 2022.

[2] G. Li, S. Liu, L. Wang, et al. "Skin-inspired quadruple tactile sensors integrated on a robot hand enable object recognition," Sci. Robot., vol. 5, no. 49, p. eabc8134, 2020.

[3] P. Wang, J. Liu, F. Hou, et al., "Organization and understanding of a tactile information dataset TacAct during physical human-robot interactions," in Int. Conf. Intell. Robots Syst., 2021, pp. 7328-7333.

[4] J. Li, Y. Liu, M. Wu, et al. "Thin, soft, 3D printing enabled crosstalk minimized triboelectric nanogenerator arrays for tactile sensing," Fundamental Research, vol. 3, no. 1, pp. 111-117, 2023.

[5] H. Park, K. Park, S. Mo, et al. "Deep neural network based electrical impedance tomographic sensing methodology for large-area robotic tactile sensing," IEEE Trans. Robot., vol. 37, no. 5, pp. 1570-1583, 2021.

[6] J. Liu, M. Wang, P. Wang, et al., "Cost-efficient flexible supercapacitive tactile sensor with superior sensitivity and high spatial resolution for human–robot interaction," IEEE Access, vol. 8, pp. 64836–64845, 2020.

[7] F. Hou, J. Liu, K. Liu, et al. "A robotic lower limb with eight dofs and whole-foot tactile perception for anthropomorphic behavior performance," in *Int. Conf. Robot. Autom*, 2022, pp. 8533-8539.

[8] K. Bae, J. Jeong, J. Choi, et al. "Large-area, crosstalk-free, flexible tactile sensor matrix pixelated by mesh layers," ACS Appl. Mater. Interfaces, vol. 13, no. 10, pp. 12259-12267, 2021.

[9] X. Zhang, X. Ye. "Zero potential method measurement error analysis for networked resistive sensor arrays," IET Sci. Meas. Technol., vol. 11, no. 3, pp. 235-240, 2017.

[10] S. Chun, J. S. Kim, Y. Yoo, et al. "An artificial neural tactile sensing system," Nature Electronics, vol. 4, no. 6, pp. 429-438, 2021.

[11] J. H. Lee, J. S. Heo, Y. J . Kim, et al. "A behavior-learned cross-reactive sensor matrix for intelligent skin perception," Adv. Mater., vol. 32, no. 22, p. 2000969, 2020.

[12] J. C. Yang, J. O. Kim, J. Oh, et al. "Microstructured porous pyramid-based ultrahigh sensitive pressure sensor insensitive to strain and temperature," ACS Appl. Mater. Interfaces, vol. 11, no. 21, pp. 19472-19480, 2019.

[13] B. Nie, R. Li, J. Cao, J. D. Brandt, and T. Pan, "Flexible transparent iontronic film for interfacial capacitive pressure sensing," Adv. Mater., vol. 27, no. 39, pp. 6055-6062, 2015.

[14] F. Han, O. Qian, G. Meng, et al. "Structurally integrated 3D carbon tube grid–based high-performance filter capacitor," Sci., vol. 377, no. 6609, pp. 1004-1007, 2022.

[15] S. Malik, K. Kishore, T. Islam, et al. "A time domain bridge-based impedance measurement technique for wide-range lossy capacitive sensors," Sensors Actuators A: Physical, vol. 234, pp. 248-262, 2015.

[16] A. U. Khan, T. Islam, B. George, et al. "An efficient interface circuit for lossy capacitive sensors," IEEE Trans. Instrum. Meas., vol. 68, no. 3, pp. 829-836, 2018.

[17] A. Kapić, A. Tsirou, P. G. Verdini, et al. "Robust analog multisensory array system for lossy capacitive sensors over long distances," IEEE Trans. Instrum. Meas., vol. 72, pp. 1-8, 2022.

[18] I. You, D. G. Mackanic, N. Matsuhisa, et al. "Artificial multimodal receptors based on ion relaxation dynamics," Sci., vol. 370, no. 6519, pp. 961-965, 2020.

[19] F. Hou, J. Liu, K. Liu, et al. "3-d-curved iontronic tactile sensor and denoising method for physical human–robot interactions," IEEE Sens. J., vol. 23, no. 7, pp. 7667-7682, 2023.

[20] J. Shi, Y. Dai, Y. Cheng, et al. "Embedment of sensing elements for robust, highly sensitive, and cross-talk–free iontronic skins for robotics applications," Sci. Advances, vol. 9, no. 9, p. eadf8831, 2023.

[21] S. Guo, J. Xiao, J. Liu, and X. Jia, "Capacitor array flexible pressure sensor design and analysis," Chin. J. Sci. Instrum., vol. 39, no. 7, pp. 49–55, 2018.

[22] S. Guo, X. Zhao, K. Matsuo, et al. "Unconstrained detection of the respiratory motions of chest and abdomen in different lying positions using a flexible tactile sensor array," [J]. IEEE Sens. J., vol. 19, no. 21, pp. 10067-10076, 2019.

[23] T. Li, k. Zheng, J. Liu, et al. "Research on operation intention based on flexible tactile sensing handle," IEEE Access, vol. 9, pp. 12362-12373, 2021.